ACOUSTICS 2012

Ultrasonic wave transport in weakly confined granular media in the intermediate frequency regime

S. Job[a], A. Strybulevych[b] and J.H. Page[b]

[a]Laboratoire d'Ingénierie des Systèmes Mécaniques et des MAtériaux, Supméca - 3, rue Fernand Hainaut - 93407 St Ouen Cedex
[b]Department of Physics and Astronomy, University of Manitoba, Winnipeg, Canada R3T 2N2
stephane.job@supmeca.fr

We present very preliminary experimental observations of ultrasonic wave transport in non-cohesive randomly close packed granular media under low confinement pressures, near the unjamming transition. The sample under experimental study is 10-mm-thick and 165-mm-diameter slabs made of 1.25-mm-diameter aluminium spheres. The slab is covered by thin plastic sheets, which allow maintaining a partial vacuum (about 0.1 atm) in the sample. Wave transport is investigated over a wide frequency range (25 kHz to 1 MHz) by analyzing the coherent ballistic transmitted field (phase and group velocities, attenuation and scattering mean free path) and the incoherent multiply scattered coda [J.H. Page et al., Phys. Rev. E, 52, 3106 (1995)]. We find that the time-of-flight intensity profile of the coda is independent of frequency over a wide range of frequencies for which the wavelength is comparable with the sizes of the scatterers. This suggests a plateau in the diffusion coefficient, as predicted by Vitelli and co-workers [Phys. Rev. E 81, 021301 (2010)].

1 Introduction

Understanding how sound propagates through random non-cohesive granular media [1,2,3,4], such as the sand, has been a challenge for many years. Due to their essentially discrete nature, wave transport in materials made of grains results from complex interplays between many physical phenomena, which lie for instance in between nonlinear elastic interactions between grains at the scale of the contacts [5,6], the existence of strong anisotropy and long range interactions along chains of force [7], and the effects of the randomness [2], order [8] and defects [9] in the fabric of a granular assembly at macroscopic scales.

Under some restrictions, for instance by considering ideal random close packing of monodisperse of elastic spheres under large external load and within the long-wavelength approximation, an effective medium theory [10] can be derived. Such a model has been shown to provide fairly satisfactory estimates of the coherent longitudinal wave velocity but unreliably overestimated values of the shear wave velocity [10]. The reason for such a failure relies on the unusual behaviors of granular media and, particularly, on the way the particles can relax to their equilibrium positions after the medium is subjected to external shear stress or strain [11].

Granular media are indeed known to exhibit very specific features, depending on whether these materials are considered to be solid structures, when the packing of grains is isostatic, or liquids or gases, when the grains are free to flow or to fly [12]. Unlike phase transitions in classical materials, the jamming/unjamming transition between solid and fluid phases occurs at zero temperature and zero applied stress in granular media [13]. The latter has important consequences for energy transport in granular media, since it implies anomalous behavior of the shear modulus near the jamming point: the ratio of shear to longitudinal wave velocities tends to zero as the confinement pressure vanishes toward unjamming of the medium [13]. According to the Debye formula, the density of shear modes, $D(\omega) \propto \omega^2/\upsilon^3$ with υ being the wave speed and ω the angular frequency, thus overwhelms the density of longitudinal modes. This leads to an excess of vibrational modes in the system, which in turn leads to an anomalous behavior of the diffusivity d [14]. Numerical simulations have indeed shown recently [14] that the diffusivity is nearly constant over a large range of frequency near the jamming transition, in strong contrast to the classical prediction in weakly scattering media, for which the diffusion coefficient (i.e. the diffusivity) decreases with frequency, $d \propto \omega^{-4}$ [15]. It is interesting to note that a similar plateau in the phonon diffusion coefficient at intermediate frequencies has been observed in porous sintered glass bead networks [16].

We present, in this proceedings paper, very preliminary experimental results on ultrasonic wave transport measurements in a sample of random close packed (RCP) monodisperse sphere under low confinement pressure. Our experimental observations are in fairly satisfactory agreement with the numerical simulations and the conclusions presented in [14]: the diffusion coefficient we estimate shows a plateau over the whole intermediate frequency range, for which the wavelength is between the thickness of our sample and the diameter of our grains.

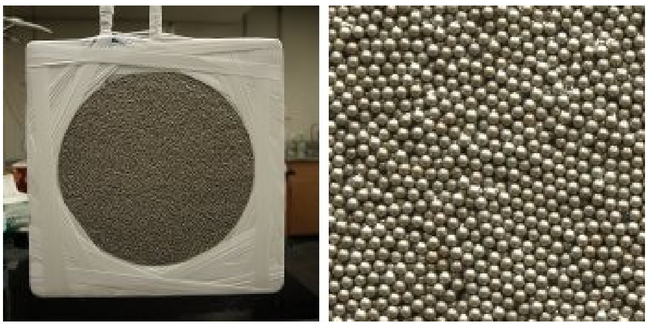

Figure 1: The sample of granular medium under study.

2 Experimental setup

The sample, shown in Fig. 1, is a circular slab placed inside a 165-mm-diameter, 10-mm-thick hole in Plexiglas holder plate. The slab is covered by a 0.05-mm-thick plastic sheet glued at the periphery on both sides of the holder. The granular medium consists of 1.25-mm-diameter non-cohesive aluminium spheres that are randomly close packed (packing fraction $\phi \approx 64\%$). The density of the sample is thus near $\rho \approx 1730\ \mathrm{kg/m^3}$. A confinement pressure is maintained on the sample: the pressure is controlled by maintaining a partial vacuum (about 0.1 atm) inside the hermetically enclosed granular slabs; our setup thus allows probing the dynamics as close as desired to the unjamming transition by diminishing the vacuum up to atmospheric pressure. Experiments presented in this proceedings paper are done in a water tank, using a plane wave ultrasonic emitter placed in the far field (about 18” away from the sample) and a hydrophone point receiver on the other side of the sample. We used several emitters to cover a wide frequency range (25 kHz to 1 MHz).

3 Ultrasonic wave experiments

In a typical experiment, an incident plane wave Gaussian pulse is emitted and reaches the sample at normal incidence, after having propagated through water. The incident pulse is multiply scattered inside the granular slab. The transmitted pressure is then recorded by the point receiver on the opposite side of the sample. The experiment is then repeated after having moved the point receiver. Finally, one obtains the total transmitted field over a large grid (21x21x4 mm in this example) centered on the axis of the sample and of the emitter. The grid covers almost one third of the cross-sectional area of the sample. Finally, the whole experiment is repeated after having removed the sample, in order to acquire a reference signal through water only. From the total transmitted pressure one can investigate wave transport from the both coherent ballistic part that travels straight through the medium without scattering out of the forward direction and from the incoherent multiply scattered part [17].

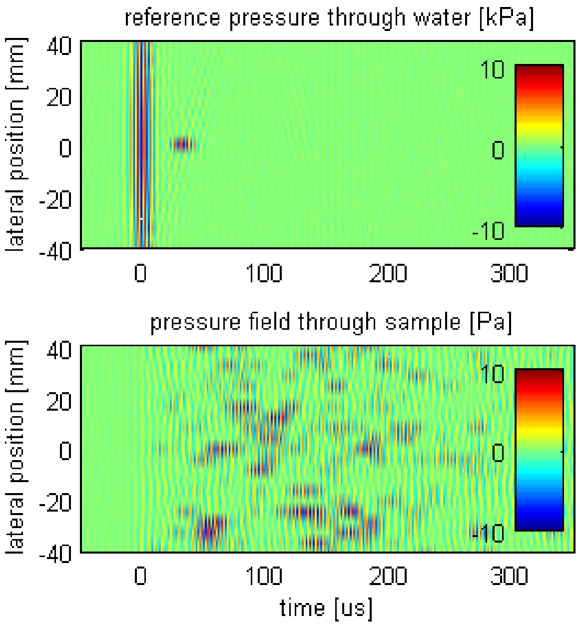

Figure 2: Reference and transmitted fields for a pulse centered on 175 kHz, along a single row of the grid.

An example of reference and transmitted pressure fields, plotted as a function of time and along a single row (for sake of clarity) of the recorded grid, is presented in Fig. 2. In this example, the incident pulse is centered around 175 kHz and has a Gaussian envelope whose duration is about five oscillations. One clearly sees in this example that the transmitted field substantially differs, both in duration and in amplitude, from the incident pulse: the very long coda and the strong attenuation reveal strong multiple scattering inside the sample.

From a set of acquisitions, recorded over a grid and for one incident central frequency, the coherent part of the transmitted signal is simply obtained by averaging the transmitted pressure over all the recorded positions. The scattered field is obtained by subtracting the coherent contribution from the total transmitted field. In Fig. 3, we plot both the coherent and the incoherent contributions obtained from the experiment shown in Fig. 2 as a function of time. For sake of clarity, the coherent contribution is plotted in red and the incoherent fields measured in several positions are all plotted in blue. The very first event of the coherent pressure represents the ballistic wave, which propagates straight through the sample. The overlay of the incoherent contribution of the transmitted pressure measured at every position on the grid reveals, in turn, that the envelope of the scattered intensity has a profile typical of a diffusive process.

From the coherent part, one can thus measure the frequency dependence of the phase and group velocities, attenuation and scattering mean free path (not detailed in this proceedings article). The scattering mean free path l is determined from the decrease with propagation distance in the intensity of the coherent field, as it acts as a source of the incoherent multiply scattered field. Measuring the attenuation of the coherent pressure intensity, $I(e)/I(0)=\exp(-e/l)$ through the sample of thickness e, yields the characteristic attenuation length, which in turn gives a reliable measurement of the scattering mean free path l, since the dissipation in the bulk of the material is negligibly small by comparison in our sample.

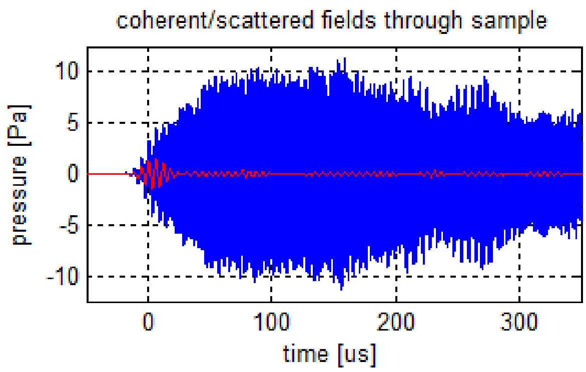

Figure 3: Coherent (red) and incoherent contributions (blue; all recorded positions) of the pressure transmitted through the sample, for a pulse centered on 175 kHz.

We present, in Fig. 4, a comparison between the reference and the transmitted coherent pulses, extracted from the measurements shown as examples in Fig. 2 and Fig. 3. In this example, the 75 dB attenuation results from strong multiple scattering: the attenuation length, i.e., the scattering mean free path, is about 0.45 times the diameter of a sphere. The time delay between the maximum of the envelope of the reference and the ballistic waves, here about 5.2 µs, indicates a wave speed of about 840 m/s. The central frequency here is 175 kHz, so that the wavelength is thus approximately 3.9 times the diameter of a sphere. The long-wavelength approximation is thus not reliably fulfilled in this example; the slight broadening of the pulse shown in Fig. 4 might reveal also a slight effect of dispersion. It is worth mentioning here that acoustic impedance $Z=\rho\times\upsilon$ of the sample matches the characteristic impedance of water within a difference of only 5%. The reflexion coefficient of longitudinal waves at normal incidence on both interfaces between water and the sample may thus safely be neglected in the analysis of the ballistic wave pulse.

In Fig. 5, we show examples of intensity envelopes of the incident and the multiply scattered waves at a few characteristic central frequencies, plotted with a semi-log scale. The intensity envelope of the multiply scattered wave (the intensity time-of-flight profile [17]) is obtained by first estimating the square of the envelope of the incoherent pressure at every recorded position of the grid, and by then averaging each of these envelopes over all the recorded positions. Assuming a frequency independent wave speed of 840 m/s, the wavelength is about 0.7 times the thickness of the sample at 125 kHz and about 1.3 times the diameter of a sphere at 500 kHz. One clearly sees in Fig. 5 that the shape of the multiply scattered intensity envelope is almost independent of frequency over this entire intermediate frequency range. For the sake of comparison, we plot in Fig. 5(d) the calculated scattered intensity flux that is predicted using the diffusion approximation with appropriate boundary conditions [17]. In this model, the time dependence of the scattered intensity profile is given by [17]:

$$I(e,t) \propto \sum_{n=1}^{\infty} A_n e^{-(\beta_n/e)^2 Dt}, \qquad (1)$$

where D is the diffusion coefficient and the coefficients A_n and β_n mainly depend on the angle-averaged internal reflection coefficient, R, on the inner sides of the sample. The shape of this curve shows a fairly reasonable agreement with our experiments over this frequency range with $D = 0.15\ \mathrm{mm}^2/\mu\mathrm{s}$ and $R = 0.85$, a value of the angle-averaged internal reflection coefficient that is similar to that estimated in aluminum bead elastic networks [18]. It is worth mentioning that this value of R is compatible with the fact that the density of shear modes exceeds the density of longitudinal modes near the jamming transition, which should in turn lead to a rather large value for R.

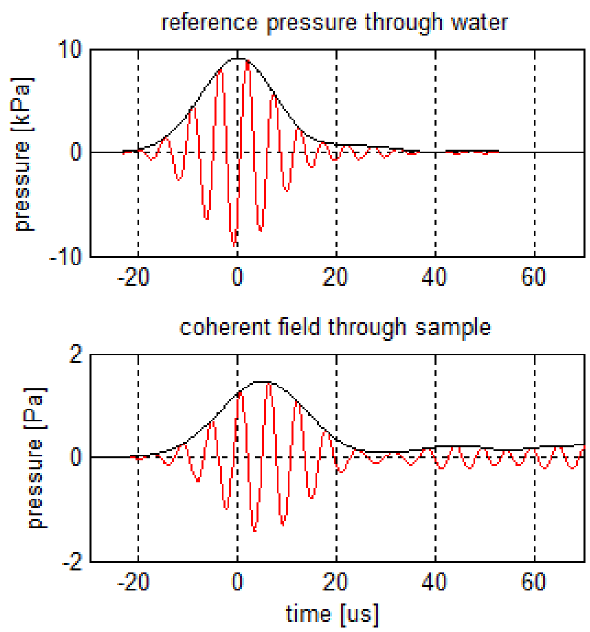

Figure 4: Reference through water (top) and ballistic wave through sample (bottom), for a pulse centered on 175 kHz

4 Conclusion

Ultrasonic wave transport through a granular medium consisting of disordered closely-packed aluminum beads under a weak confining pressure exhibits very strong multiple scattering in the intermediate frequency regime. Despite this very strong scattering, the weak ballistic pulse that propagates coherently through the sample was extracted, giving information on the phase velocity and scattering mean free path. The time dependence of the dominant multiply scattered component of the total transmitted intensity was also measured and compared with predictions of the diffusion approximation. In this intermediate frequency regime, the intensity time-of-flight profiles are essentially independent of frequency, implying that the diffusion coefficient exhibits a frequency–independent plateau, consistent with recent predictions for energy transport in granular media by Vitelli and co-workers [14].

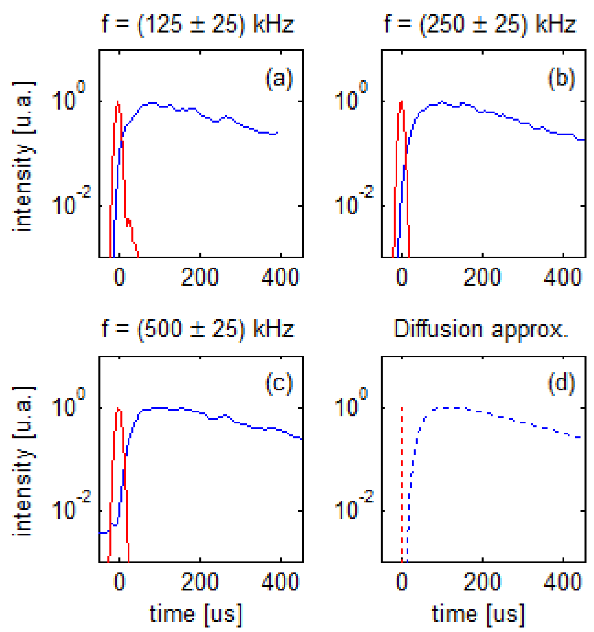

Figure 5: Incident (red) and scattered intensity (blue) as a function of time for an incident plane wave centered at (a) 125 kHz, (b) 250 kHz and (c) 500 kHz. Fig. (d) corresponds to Eq. (1) with $D = 0.15\ \mathrm{mm}^2/\mathrm{us}$ and $R = 0.85$.

Acknowledgments

S.J. is grateful for the financial support received from the French *Agence Nationale de la Recherche* (ANR-CONICYT #011; *MicMacGrains*) and from the *Ultrasonic Research Laboratory*, during his sabbatical stay at the University of Manitoba (Canada).

References

[1] C.H. Liu and S.R. Nagel, "Sound in sand", *Phys. Rev. Lett.* 68(15), 2301 (1992)

[2] C.H. Liu and S.R. Nagel, "Sound in granular material: Disorder and nonlinearity", *Phys. Rev. B* 48, 15646 (1993)

[3] X. Jia, C. Caroli and B. Velicky, "Ultrasound propagation in externally stressed granular media", *Phys. Rev. Lett.* 82, 1863 (1999)

[4] V. Tournat, V.E. Gusev, and B. Castagnède, "Influence of ballistic to diffusion transition in the primary wave propagation on parametric antenna operation in granular media", *Phys. Rev. E* 66, 041303 (2002)

[5] H. Hertz, "Über die berührung fester elastischer körper", *J. Reine Angew. Math.*, 92, 156 (1881)

[6] J. D. Goddard, "Nonlinear Elasticity and Pressure-Dependent Wave Speeds in Granular Media", *Proc. R. Soc. Lond. A* 430(1878), 105 (1990)

[7] T. Travers, M. Ammi, D. Bideau, A. Gervois, J. C. Messager, and J. P. Trodec, "Uniaxial Compression of 2d Packings of Cylinders. Effects of Weak Disorder", *Europhys. Lett.* 4, 329 (1987)

[8] V.F. Nesterenko, "Propagation of nonlinear compression pulses in granular media", *J. Appl. Mech. Tech. Phys.* 24, 733 (1984)

[9] S. Job F. Santibanez, F. Tapia and F. Melo, "Wave localization in strongly nonlinear Hertzian chains with mass defect", *Phys. Rev. E* 80, 025602(R) (2009)

[10] H.A. Makse, N. Gland, D.L. Johnson and L. Schwartz, "Granular packings: Nonlinear elasticity, sound propagation, and collective relaxation dynamics", *Phys. Rev. E*, 70, 061302 (2004)

[11] C.S. O'Hern, L.E. Silbert, A.J. Liu and S.R. Nagel, Jamming at zero temperature and zero applied stress: The epitome of disorder, *Phys. Rev. E* 68, 011306 (2003)

[12] H.M. Jaeger, S.R. Nagel and R.P. Behringer, "Granular solids, liquids, and gases", *Rev. Mod. Phys.* 68, 1259 (1996)

[13] A.J. Liu and S.R. Nagel, "The Jamming Transition and the Marginally Jammed Solid", *Annu. Rev. Condens. Matter Phys.* 1, 347 (2010)

[14] V. Vitelli, N. Xu, M. Wyart, A.J. Liu and S.R. Nagel, "Heat transport in model jammed solids", *Phys. Rev. E* 81, 021301 (2010)

[15] P. Sheng, "Introduction to wave scattering, localization and mesoscopic phenomena", Academic Press, San Diego, CA, USA (1995)

[16] J.H. Page, W.K. Hildebrand, J. Beck R. Holmes and J. Bobowski, "Phonons in porous media at intermediate frequencies", *Phys Stat. Sol* (c), 1, 2925 (2004).

[17] J.H. Page, H.P. Schriemer, A.E. Bailey and D.A. Weitz, "Experimental test of the diffusion approximation for multiply scattered sound", *Phys. Rev. E* 52, 3106 (1995)

[18] H. Hu, A. Strybulevych, J.H. Page, S.E. Skipetrov and B.A. van Tiggelen, "Localization of ultrasound in a three-dimensional elastic network", *Nature Physics*, **4**, 945, (2008).